Effect of starting powder particle size and heating rate on spark plasma sintering of Fe-Ni alloys

M.B Shongwe[a,†], M.M Ramakokovhu[a], S Diouf[a], M.O Durowoju[a], B.A Obadele[b], R. Sule[a], P.A Olubambi[b], E.R Sadiku[a]

[a]Institute for NanoEngineering Research, Department of Chemical, Metallurgical and Materials Engineering, Tshwane University of Technology, Pretoria, South Africa

[b]Department of Chemical Engineering Technology, University of Johannesburg, Johannesburg, South Africa

ABSTRACT

The effect of starting powder particle size and heating rate on spark plasma sintering of Fe-Ni alloys was investigated, with the particle powder size varying from 3 to 70 μm and heating rate from 50 to 150 °C/min. The effect of the starting powder particle size was more obvious when comparing 3-FeNi and 70-FeNi at all heating rates, with the former having better density and hardness than the latter. Sintered densities close to theoretical (≥ 99%) were achieved for a heating rate of 50°C/min for the different starting particle size powders, and decreased with increasing heating rate. The average grain size of alloys sintered at 150°C/min was ~34% smaller than those sintered at 50°C/min. The porosity content of the sintered samples increased with increasing heating for the same particle size. The shrinkage rate depends on both heating rate and particle size. At a particle size of 3 μm and a heating rate of 50°C/min, three peaks were observed indicative of the phenomena responsible for good densification. As the heating rate increases, only two peaks and one peak are observed at heating rates of 100 and 150°C/min, respectively. This suggests that, unlike high heating rates, the longer processing time at low heating rate allows the three phenomena to take place. The hardness measurement revealed a steady decrease with increasing heating rate. At a heating rate of 150°C/min the particles were well packed but no typical dimple structure of a ductile material was observed. However, for samples sintered at 50 and 100°C/min a typical dimple fracture morphology was observed.

Keywords: Densification, Sintering, Microstructure, Hardness, Fracture.

[†]Corresponding author. Tel: +27 12 382 5488, E-mail address: ShongweMB@tut.ac.za, m.shongwem@gmail.com (M.B. Shongwe, PhD).

1. Introduction

Fe-Ni alloy, as a soft magnetic material with high permeability and low coercivity in weak magnetic field, is widely applied in industrial engineering, electronics, fuel injection system components and electrical industry. Conventional soft magnetic alloys were fabricated by the methods of casting and machining. However, with the conventional processing method of Fe-Ni alloys fabrication it's hard to elaborate parts with complex shape and to obtain perfect magnetic properties due to work hardening of Ni element [1-3]. Numerous researchers have studied the properties of Fe–Ni fabricated by powder injection molding (PIM) [4-6], Metal injection molding (MIM) [7-10] and laser fabrication such as selective laser melting/selective laser sintering (SLM/ SLS) [11, 12] which have been reported to be near-net shaping techniques that are particularly advantageous for applications where complex shapes with high dimensional accuracy and high density are required. For many applications in electronic devices, a solid, high density material is needed. However, the classic sintering techniques lead to a rapid grain growth, thereby losing the unusual magnetic and mechanical properties associated with very fine grains. A promising novel technique to consolidate powders into high density solids with a controlled grain size is spark plasma sintering (SPS) [13]. However, so far, work on Fe-Ni alloys fabricated by spark plasma sintering system has been rarely reported.

Currently, Spark Plasma Sintering (SPS) technology for high-speed compaction is widely used in powder material engineering [14]. In SPS technology, a conductive die is used, into which raw powder materials are loaded. Mechanical pressure (20-100 MPa) is applied to the die along the vertical axis, and a pulsed electric current of low voltage (approximately 4-20 V) and high amperage (0.5-40 kA) is passed through the die. The sintering temperature is controlled using a thermocouple or an optical pyrometer, which is located at the outer wall of the die [15]. The SPS method has demonstrated its high efficiency in consolidating ceramic and metal nanomaterials, composites, solid materials (Table 1), functionally graded materials, composite materials based on carbon nanotubes and nanofibers, electronic materials, thermoelectrics and bio-materials [14-22]. The SPS method has several advantages that distinguish it from the traditional sintering methods such as hot pressing and sintering of pre-compacted billets without pressure. Specifically, SPS enables a reliable control of the sintering process parameters and material's microstructure. The method is distinguished by low power consumption and high performance [14-16]. It should be noted that SPS sintering

of samples usually requires much less time than the conventional methods, and studies show that the SPS sintering temperature is almost always lower than that in the conventional methods [16].

Recently, Shongwe *et al.* [23] demonstrated that spark plasma sintering can offer a potentially viable means to consolidate Fe-Ni alloys for higher performance applications, however the work was not focused on optimising parameters that affect the resultant alloy properties such as heating rate and also the effect of starting powder particle size and no work could be found in literature focusing on this aspect. As a result, this paper is focused on the effect of starting powder particle size and heating rate on the microstructure and mechanical properties of Fe-Ni alloys sintered using HHPD-25 SPS system from FCT Germany. The microstructural features, fractography and mechanical properties were analysed; moreover the reasons behind the microstructural developments were explained.

2. Experimental procedure

2.1. Powders preparation

One commercial Fe and Ni as-received mixed powders and three elemental Fe and Ni of 99.5% purity with particle sizes of 70, 44, 8 and 3 μm, respectively, were used as starting materials, and the characteristics are summarized in **Table 1**. The 70 μm sizes were received in mixed form, while the rest of the powders were received separately without mixing. The three different particle size powders were mixed using the Turbula Shaker Mixer T2F. An optimum mixing speed of 49 rpm and mixing time of 5h were used. A 250 ml cylindrical plastic vessel with a powder fill level of 10% was loaded axially, placed in the mixing chamber and subjected to translational and rotational motions. The mixing was carried out in a dry environment. The morphology of the powders was then examined with a field emission scanning electron microscopy (FESEM, JSM-7600F, Jeol, Japan) equipped with energy dispersive X-ray spectrometer (EDS). **Fig. 1** shows the as-received and the other three mixed powders with the as-received showing mainly regular spherical particles and negligible agglomeration typical of atomized powders, while the rest mixed powders show irregular shapes and slight agglomeration. In this paper the powders are denoted by the maximum particle sizes, as x-FeNi, where x is the maximum particle size for the Fe-44%Ni alloy.

Table 1

Characteristics of the Fe-44%Ni powders.

Elemental powder	Purity (%)	Particle Size			Main impurity (wt.%)			
		Fe	Ni	Mixture	C	O	P	N
Fe-44%Ni	99.5	-	-	≤70	≤0.002	≤0.07	0.0008	-
Fe-44%Ni	99.5	44	25	≤44	≤0.05	≤0.11	0.0003	-
Fe-44%Ni	99.5	5	8	≤8	≤0.02	≤0.01	0.0012	-
Fe-44%Ni	99.5	3	0.5	≤3	≤0.09	≤0.08	0.0003	-

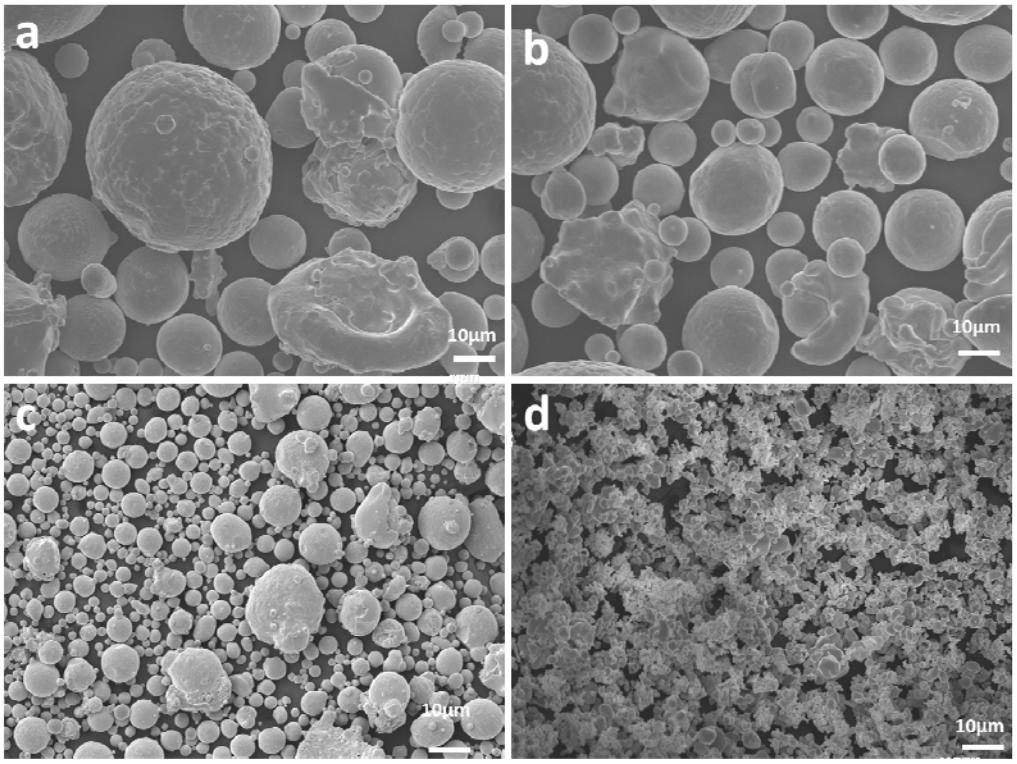

Fig. 1. SEM morphology of the as-received: (a) 70-FeNi, and mixed powders (b) 44-FeNi (c) 8-FeNi and (d) 3-FeNi.

2.2. Sintering

The mixed powders were sintered by SPS (HHPD-25 Sytem from FCT GmbH Germany) in a 30 mm-inner-diameter graphite die. Graphite foils of 0.2 mm thickness were placed between the punches and the powders, and between the die and the powders for easy removal and significant reduction of temperature inhomogeneities. In addition, the exterior of the die was covered by a porous graphite felt with a thickness of ~10 mm, which was used as a thermal insulation to reduce the radiation loss and possible temperature gradient [24,25]. Sintering

was performed in vacuum and a constant pressure of 30 MPa was applied from the beginning of the heating step to the end of the dwell. For all the sintering experiments, heating schedules were controlled by a preset heating program with full details shown in **Table 2**. When the required temperature and holding time was reached the electric current was shut off, the applied stress released, and the specimens were immediately cooled down in the furnace. The sintering temperature was measured by an optical pyrometer which was implanted in the SPS apparatus at 3 mm from the top of the sample surface. Discs of 30 mm diameter of approximately 5 mm in height were produced.

Table 2

Sintering schedules to consolidate blended powders

	Sintering conditions		
Alloy	Heating rate (°C/min)	Reference temperature (ºC)	Dwell duration (min)
Fe-44%Ni	50	1100	2
	100	1100	2
	150	1100	2

2.3. Density and microstructural characterization

All of the sintered specimens were ground and polished to remove any surface graphite contamination. Then the density of the sintered specimen was determined by the Archimedes principle. The relative density was calculated with reference to the theoretical density of the starting powders constituents using the rule of mixtures. The microstructure of specimens taken from the polished surface or fracture surfaces at cross sections (parallel to the acting force) of the sintered bodies was examined by SEM (FESEM, JSM-7600F, Jeol, Japan) incorporated with an EDX detector (Oxford X-Max) with INCA X-Stream2 pulse analyzer software, and back scattered electron detectors. The INCA analyzer software was set to 70 s acquisition time and at a process time of 2 s. The polished specimens were chemically etched with a 6% nitric solution for 15 s to observe the microstructure and measure the grain size. Focus was given on studying the microstructure at different regions along the cross section. To avoid the influence of near-surface effects and some other uncertain factors, only the cross section of the specimen was used for examination. The phases present in the sintered specimen were characterized by X-ray diffraction (XRD) using a PANalytical Empyrean

model with Cu Kα radiation and analyzed using Highscore plus software. The XRD analysis was carried out on the section perpendicular to uniaxial pressed direction.

2.4. Mechanical property measurement

The microhardness of the samples was measured using a Future-tech Vickers microhardness tester at a load of 100 gf (1.0 N) (HV1) and dwell time of 10s. The test result for each sample was the arithmetic mean of ten successive indentations with standard deviations.

3. Results and Discussion.

3.1 Densification and Microstructural variations

3.1.1 Density measurement

Comparison of the sintered density for the different conditions is shown in **Fig. 2**. Sintered densities close to theoretical (≥ 99%) were achieved for a heating rate of 50°C/min for the different starting particle size powders. Past research has shown densification is a prerequisite for adequate mechanical properties [26]. Thus, it is expected that the samples sintered at a heating rate of 50°C/min will possess better mechanical properties. For the 44-FeNi and 8-FeNi alloys the effect of the particle size is very small on the relative density, and in fact at a heating rate of 150°C/min the relative density is the same and is 98.6%. The effect of the starting powder particle size is more obvious when comparing 70-FeNi and 3-FeNi at all heating rates. This is not surprising since the size range is much bigger to pick up its influence on the density. As the heating rate is increased from 100 to 150°C/min, its effect becomes more pronounced on the relative density as it drops considerably (≤ 99%) for all the alloys. This is due to the fact that at high heating rates uniformization of particle size through grain growth is discouraged since the process is much quicker and this results in few sintering necks and there by increases porosity and poor packing of the particles.

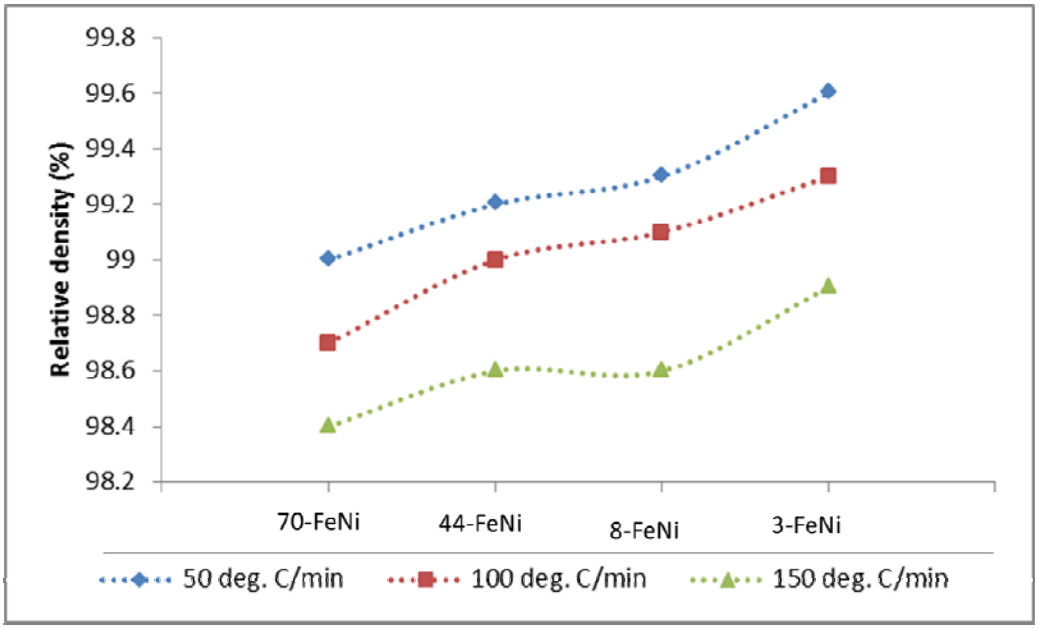

Fig. 2. Effect of starting powder particle size and heating rate on the relative density of Fe-44%Ni alloys.

3.1.2 Effect of heating rate and powder particle on grain size

The progressive evolution of microstructures in different regions of the sample manufactured using varying powder particle size and heating rates is shown in Fig. 3. All the microstructures were taken at low and similar magnification in order to ensure that the grains distribution and size is captured. There are relatively different arrangements of the grains in the alloys, which respectively designate the variation in densification. In all of the alloys, the microstructure shows that the fine grains of the starting powder particles (Fig. 1) is replaced by sintered particles in which some grain growth has taken place as seen in Fig. 3, which is more pronounced at the lowest heating rate. The comparison of the microstructures for the different particle sizes at the same heating rate, show that there is little difference in the particle size with varying powder particle size, except when the 77-FeNi alloy is compare with the 3-FeNi which shows a difference in the particle size. The results confirm that heating rate has a profound effect on the final grain size compared to the starting powder particle size, and this is similar to the observation on the effect of powder particle size on relative density (Fig. 2). As the heating rate is increased from 50 to 100°C/min the grain size slightly decreases. A further increase of the heating rate up to 150°C/min in all of the alloys results in a further drop in the particles' size, with a few sintering necks, indicating decreased densification. This is an indication that the high heating rate could not provide sufficient time for homogenization of the microstructure and allow improvement of the alloys packing

density. As pointed out by Song *et al.* [27], neck growth depends on the local distribution of the current density and a self-adjusting mechanism leads to a final homogeneous distribution of necks. The linear intercept method was used to determine the grain size for the different alloys at different heating rates (Fig. 4). The average grain size of alloys sintered at 150°C/min is 34% smaller than those sintered at 50°C/min and the relative density was decreased at 150°C/min mainly due to the poor necking between the grains although the grains were finer. These results illustrate that grain growth, pores reduction and increase in density are simultaneous processes.

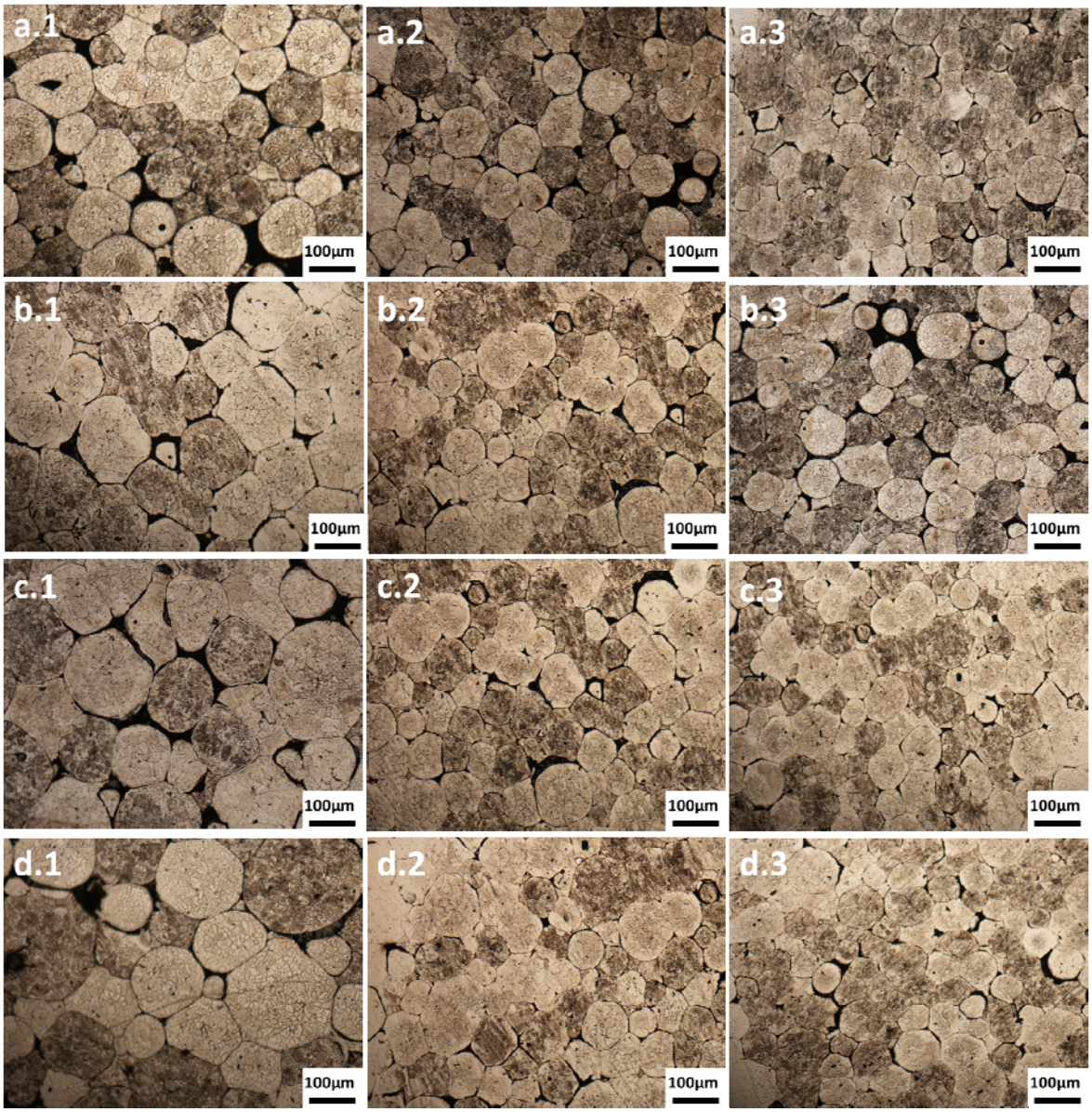

Fig. 3. SEM micrographs of the Fe-44%Ni alloy showing the microstructural evolution of the samples with different starting particle size: (a) 70-FeNi, (b) 44-Fe-Ni, (c) 8-FeNi and (d) 4-FeNi where 1 = 50-°C/min, 2 = 100-°C/min and 3 = 150°C/min.

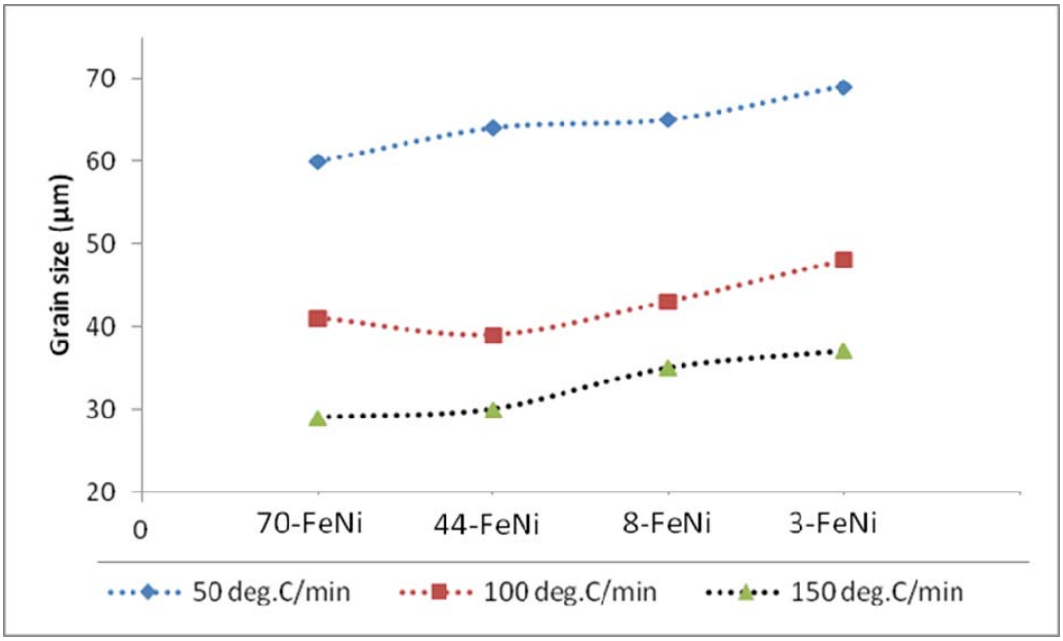

Fig. 4. Effect of starting powder particle size and heating rate on the grain size of Fe-44%Ni alloys.

3.1.3 Effect of heating rate and powder particle on pore content and size

The microstructures obtained by SEM from cross-sections of the sintered Fe-Ni alloys with varying heating rate and starting powder particle size are shown in Fig. 5 indicating the pore size. Using these microstructures and ImageJ analysis software, the amount of porosity of the samples were determined. The porosity content of the sintered samples depends on the heating rate and increased with increasing heating for the same particle size (Fig. 6), this is evident from the SEM images (Fig. 5) particular when the 50°C/min is compared with the 150°C/min heating rate. With a heating rate of 50°C/min the lowest level of porosity content was obtained in all the samples. Under the same heating rate and varying starting powder particle size, it was not possible by visual observation of the SEM images to notice the effect of starting powder particle size on the porosity content; however image analysis indicates a minor variation between the smallest particle size and the largest particle size. The microstructures indicate that with increasing heating rate more grain boundaries are observed. This was expected since the lower the heating rate, grains have enough time to form sintering necks, which grow and eliminate by combining with other grain boundaries to eliminate multiple grains. The high porosity values of all the samples compared to the measured density by the Archimedes method is due to the fact that in ImageJ the grains and also over-

etched grain boundaries are taken as porosity, and as a result the porosity is over-estimated leading to results with systematic errors.

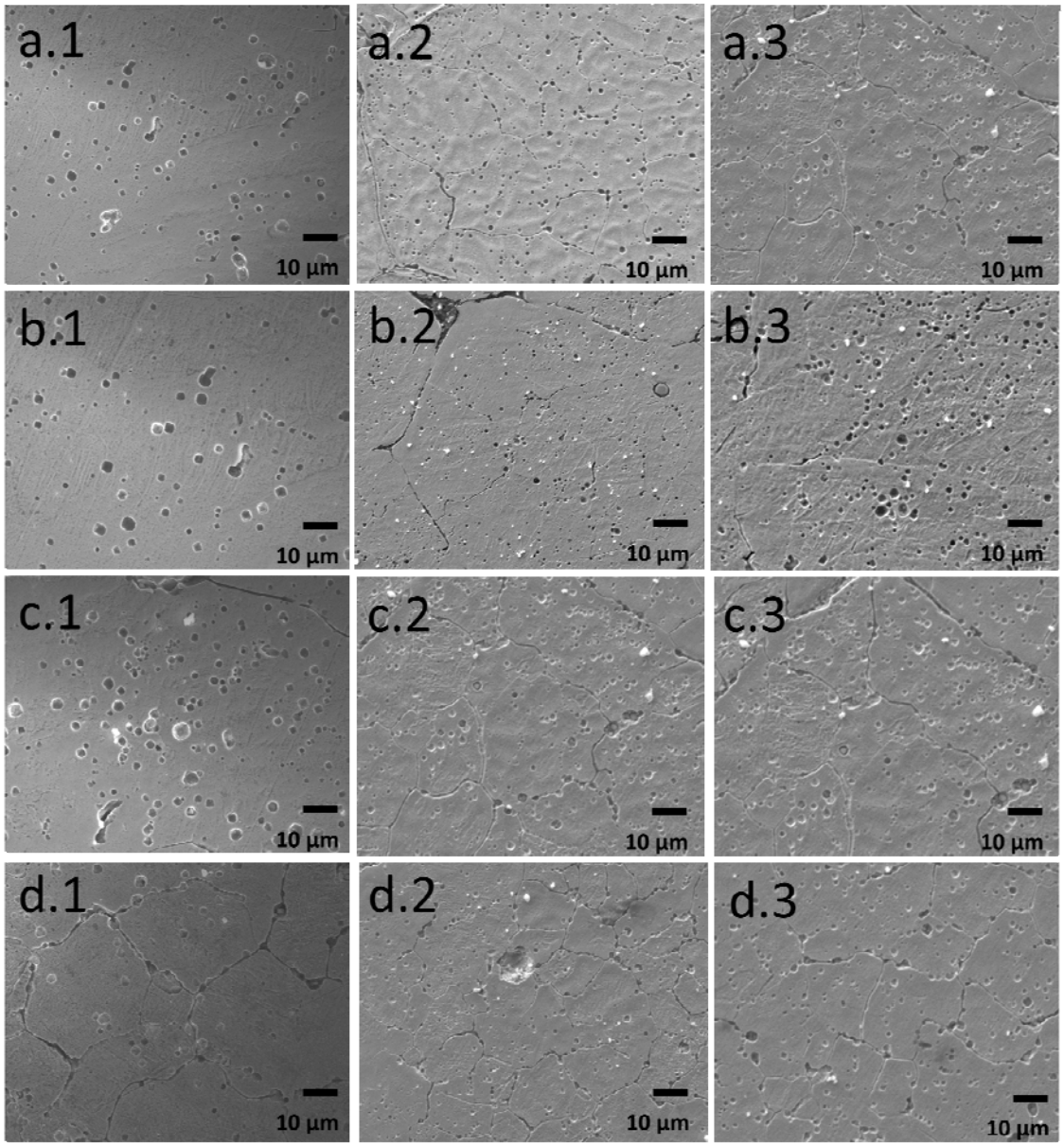

Fig. 5. SEM micrographs of the Fe-44%Ni alloy showing the porosity content of the samples with different starting particle size powders: (a) 70-FeNi, (b) 44-Fe-Ni, (c) 8-FeNi and (d) 4-FeNi where 1 = 50 °C/min, 2 = 100 °C/min and 3 = 150 °C/min.

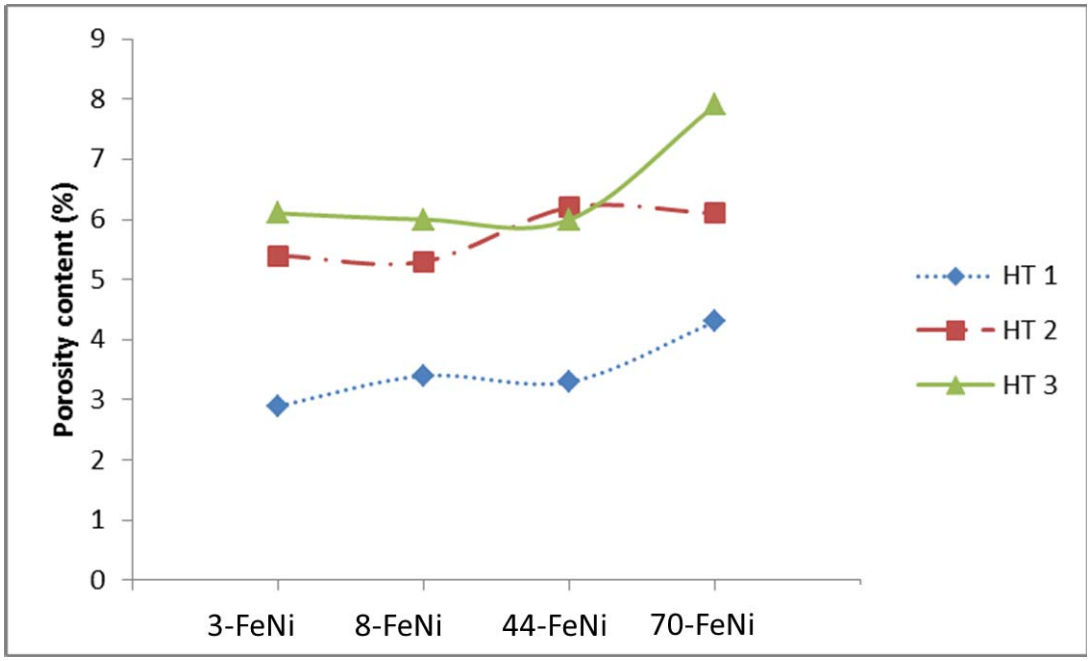

Fig. 6. Effect of starting powder particle size and heating rate on porosity content of Fe-44%Ni alloys.

3.1.4 Densification and sintering phenomena

The relative piston travel (displacement) can be used as an indirect measure of densification during spark plasma sintering. The displacement indicates changes in the thickness of a specimen as a result of punches movement against the die with time. The displacement towards negative or positive direction could mean expansion or shrinkage respectively [28]. The shrinkage rate and sintering time at different heating rate during SPS processing have been used to explain the densification behaviour of sintered ceramic material [29]. Effort is made in this study to examine the effect of heating rate on the densification of mechanism of Fe-Ni alloys samples. Figure 7 show the shrinkage rate versus time of the sintered samples. As it can be seen from Figure 7, the shrinkage rate depends on both heating rate and particle size. At a particle size of 3 μm and a heating rate of 50^{o}C/min, three peaks are clearly observed. These peaks are indicative of the phenomena responsible for densification: rearrangement of the particles, localized deformation at the contact points, bulk deformation of the particles [30, 31]. As the heating rate increases, only two peaks and one peak are observed at heating rates of 100 and 150^{o}C/min, respectively. This suggests that, unlike high heating rates, the longer processing time at low heating rate allows the three phenomena to take place. At a heating rate of 100^{o}C/min, an increase in particle size results in a continuous

delay of the first peak and the overlapping of the two peaks at a particle size of 70 µm. This is possibly due to the model proposed by Song et al. [27], the high overheating at the particle surface for bigger particles. The same behaviour can be observed for the four different cases. An increase in particle size results in an overlapping of the phenomena and a decrease of the intensity of the peaks. In all the samples produced, the maximum shrinkage rate was observed at 50ºC/min. It can be observed that the samples sintered with heating rates of 50 and 100ºC/min yield a relatively high density and hardness values, respectively compared to that of 150ºC/min as shown in Figs 2 and 5.

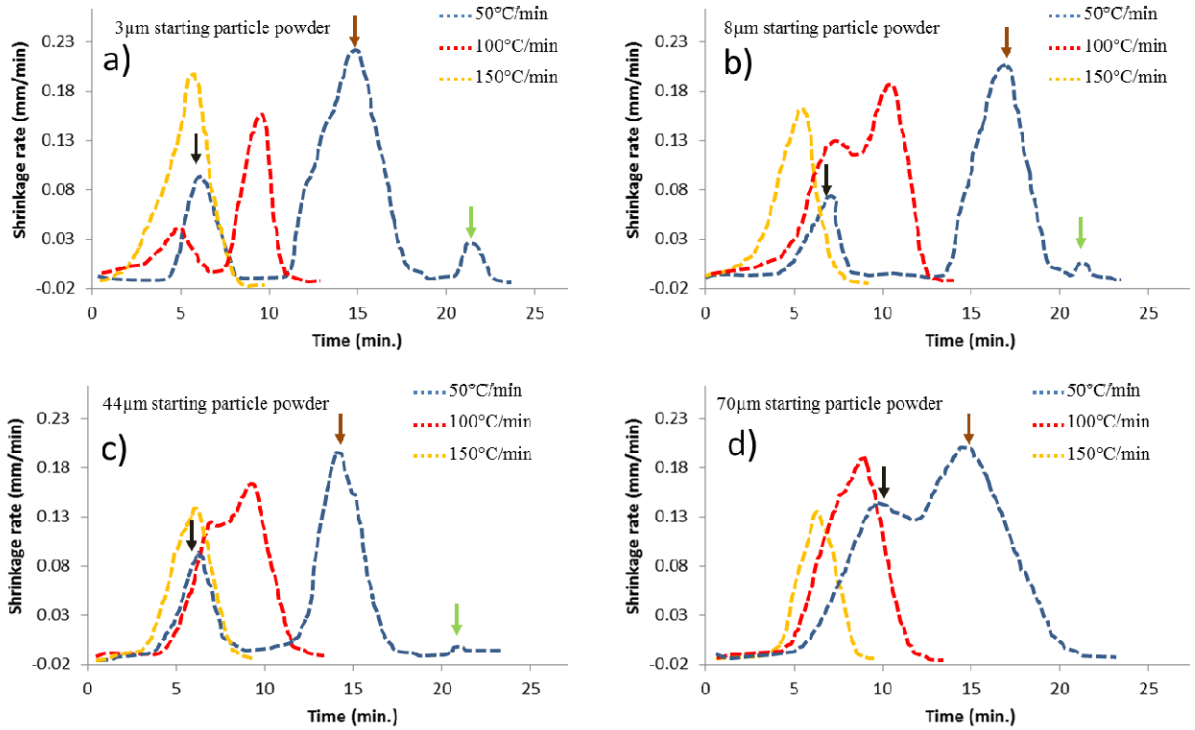

Fig. 7. Shrinkage rate versus time for the Fe-44%Ni alloys sintered at 1100°C with varying starting particle powder size and heating rate, also illustrating the densification mechanisms taking place: black arrow – particle rearrangement, brown arrow - localized deformation at the contact points and green arrow - bulk deformation of the particles.

3.2 Mechanical properties and fractography

The grain size critically influences the mechanical properties of high strength materials [32]. Previous studies have shown that the mechanical properties of materials depend on temperature [32]. Therefore, effort was made in this study to investigate the influence of powder particles on microhardness. Table 3 summarizes the Vickers hardness value of the specimen in relation to the heating rate. It was observed that the microhardness of sintered

samples decreases with increase in powder particle size. On the other hand, the microhardness of the samples was found to reduce with increase in the heating rate. From the results obtained, it could be stated that that hardness of Fe-Ni at different sintering temperatures can be influenced by the size of the starting powders, distribution of the phases and porosity at elevated temperatures. Fig. 8 shows the influence of powder particles size and heating rate on hardness of the sintered samples. The microhardness values of the sample with 3µm powder particles sintered at 50, 100 and 150ºC/min were found to be 275 HV, 255 HV and 220 HV, respectively. The results of the hardness measurement for the other samples also reveal a steady decrease in microhardness value with increase in heating rate.

Table 3: Vicker's hardness of specimen and their heating rate

samples	**Heating rate, ºC/min**	**Hardness HV_1**
3FeNi	50	275
3FeNi	100	255
3FeNi	150	220
8FeNi	50	278
8FeNi	100	249
8FeNi	150	189
44FeNi	50	263
44FeNi	100	265
44FeNi	150	195
70FeNi	50	259
70FeNi	100	240
70FeNi	150	180

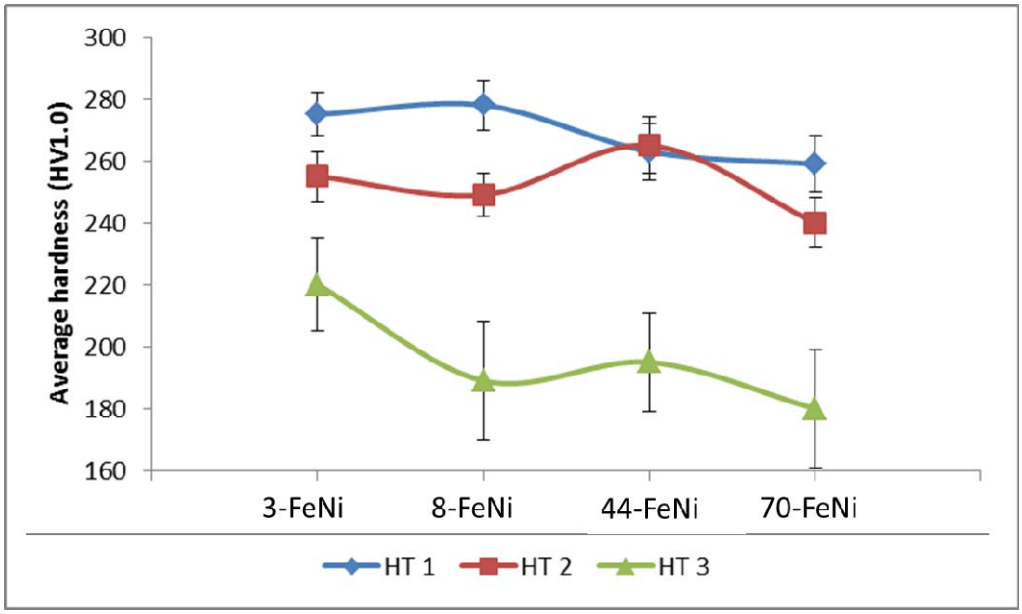

Fig. 8. Effect of starting powder particle size and heating rate on Vickers' microhardness (HV1.0) of Fe-44%Ni alloys.

Fig. 9 shows the fractography of the sintered samples at different heating rates. The sample sintered at 150°C/min revealed that the particles are well packed but no typical dimple structure of ductile material was observed (Fig. 9 (a.3). However, typical dimple fracture morphology was observed in the sample sintered at 50 and 100°C/min as shown in Fig. 9 (a.1 and a.2) which suggests the occurrence of sintering. The results of hardness value obtained could be better explained with the fracture surface. The low hardness value obtained in samples sintered with 150°C/min (Fig. 8) could also be due to weak bonds between the powder particles which resulted from poor sintering of the samples. It can be observed that no dimple structure was found in samples with higher powder particle size sintered at 50 and 100°C/min as shown in Fig. 9 (c.1 to c.3 & d.1 to d.3). It could be deduced that the amount of neck formation depends on the particle size as well as the heating rate. This observation is reasonably consistent with the report presented by Shen et al. [29] on the spark plasma sintering of alumina. On those studies, it was stated that neck formation depends on the particle size of the precursor powder, the green body density, the applied pressure and the heating rate.

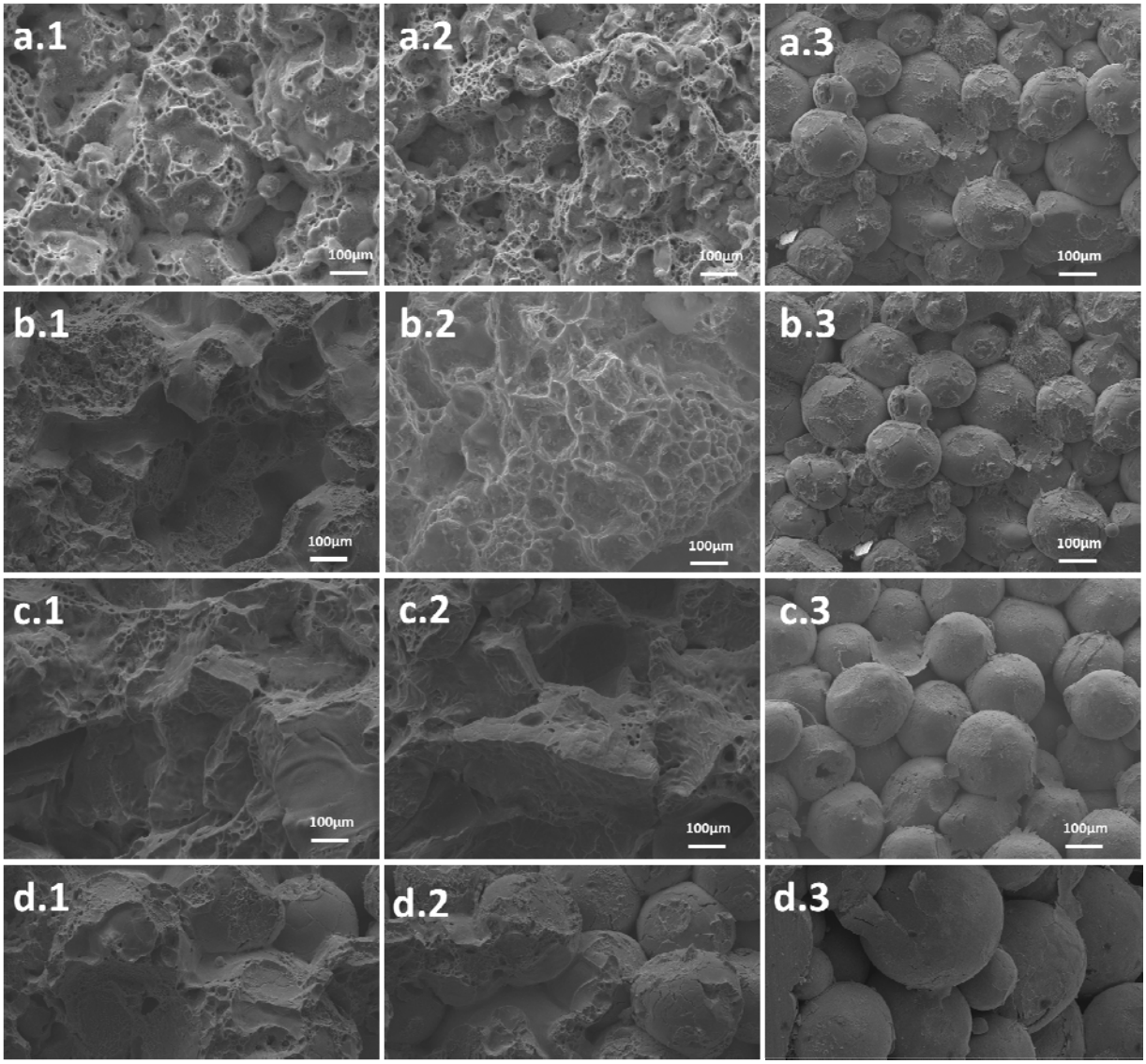

Fig. 9. Fractograph of FeNi samples with different starting particle size powders: (a) 3-FeNi, (b) 8-Fe-Ni, (c) 44-FeNi and (d) 70-FeNi where 1 = 50°C/min, 2 = 100°C/min and 3 = 150°C/min.

4. Conclusions

Effect of heating rate and powder particle size on the mechanical properties of Fe-Ni has been investigated using scanning electron microscopy (SEM) and Vickers microhardness test. The effect of starting powder particle size on the hardness was evident for the smallest size compared with the largest particle size, with the former having a high hardness than the latter at all heating rate conditions. The hardness of the samples decreases with an increase in